Geochemistry Geophysics Geosystems G3
AN ELECTRONIC JOURNAL OF THE EARTH SCIENCES
Published by AGU and the Geochemical Society

Article
Volume 10, Number 7
11 July 2009
Q07003, doi:10.1029/2009GC002450
ISSN: 1525-2027

Environmental change in the subtropics during the late middle Eocene greenhouse and global implications

Chioma U. Okafor
Department of Geology and Geophysics, Texas A&M University, College Station, Texas 77843, USA

Deborah J. Thomas
Department of Oceanography, Texas A&M University, College Station, Texas 77843, USA (dthomas@ocean.tamu.edu)

Bridget S. Wade
Department of Geology and Geophysics, Texas A&M University, College Station, Texas 77843, USA

John Firth
Integrated Ocean Drilling Program, College Station, Texas 77845, USA

[1] Oxygen isotope records from ODP Site 1052 (Blake Nose, subtropical North Atlantic Ocean) indicate significant short-term, high-amplitude variability (up to 1.4‰ in about 2500 to 4000 years) during the late middle Eocene (37.9–37.5 Ma). These variations reflect a combination of changes in sea surface temperature and the oxygen isotope composition of the regional seawater. In order to independently evaluate the magnitude of SST changes at Blake Nose and better understand the nature of environmental change during the late middle Eocene, we present planktonic foraminiferal Mg/Ca data combined with $\delta^{18}O$ data from the same samples. The calculated Mg/Ca paleotemperatures indicate a decrease in SSTs over the study interval from ~33 to 28°C at the same time that previously published foraminiferal $\delta^{18}O_{calcite}$ values from the same samples also decrease. Thus, the $\delta^{18}O_{calcite}$ values must reflect a significant component of seawater $\delta^{18}O$ change in order to reconcile the opposite paleotemperature trends reflected by both proxies. Calculated $\delta^{18}O_{seawater}$ values decreased from ~3‰ at 37.83 Ma to ~2‰ at 37.6 Ma. The combined trends of the SST and $\delta^{18}O_{seawater}$ cannot be explained by an increase of continental ice over this time interval. Instead, the data favor an overall weakening of the hydrological cycle as global climate transitioned from the greenhouse to icehouse.

Components: 7950 words, 3 figures, 1 table.

Keywords: Ocean Drilling Program; middle Eocene; paleoceanograpy.

Index Terms: 1065 Geochemistry: Major and trace element geochemistry; 4901 Paleoceanography: Abrupt/rapid climate change (1605).

Received 23 February 2009; **Revised** 13 April 2009; **Accepted** 3 June 2009; **Published** 11 July 2009.

Okafor, C. U., D. J. Thomas, B. S. Wade, and J. Firth (2009), Environmental change in the subtropics during the late middle Eocene greenhouse and global implications, *Geochem. Geophys. Geosyst.*, *10*, Q07003, doi:10.1029/2009GC002450.

1. Introduction

[2] Geochemical, paleontological, and sedimentological data indicate that the early Eocene was the warmest interval of the Cenozoic [e.g., *Wolfe*, 1980; *Adams et al.*, 1991; *Zachos et al.*, 1994]. Temperatures during peak Eocene warmth at ~50 Ma were as high as 18°C at high latitudes and >30°C at low latitudes [e.g., *Burgess et al.*, 2008; *Sluijs et al.*, 2008; *Pearson et al.*, 2007] suggesting little or no ice at the poles and a reduced equator-to-pole gradient compared to the modern. Following the early Eocene peak warmth, global temperatures declined, culminating in the expansion of ice sheets in Antarctica by the earliest Oligocene [e.g., *Miller et al.*, 1991; *Zachos et al.*, 1996, 2001; *Lear et al.*, 2000; *Coxall et al.*, 2005].

[3] Oxygen isotope records from high, middle and low latitudes indicate high-amplitude variations on orbital and suborbital time scales during the Eocene cooling trend [e.g., *Diester-Haass and Zahn*, 1996; *Bohaty and Zachos*, 2003; *Wade et al.*, 2001; *Wade and Kroon*, 2002]. In the Southern ocean, *Diester-Haass and Zahn* [1996] reported short-term fluctuations with periodicities of 100–400 ka in benthic foraminiferal stable isotope and abundance data from the Eocene-Oligocene (45–26 Ma) interval of ODP Site 689, Maud Rise, Weddell Sea. *Bohaty and Zachos* [2003] and *Bohaty et al.* [2009] generated high-resolution stable isotope records from the middle Eocene (49–34 Ma) of Kerguelen Plateau and Maud Rise (ODP Sites 689, 690, 744, 748 and 738) and found a distinct negative $\delta^{18}O$ excursion (~1‰) at 40.0 Ma (now known as the middle Eocene Climatic Optimum) in the middle of the prominent long-term Eocene cooling trend.

[4] In the subtropical North Atlantic (Blake Nose; Figure 1), *Wade and Kroon* [2002] found evidence of significant variability in the oxygen isotope records from late middle Eocene mixed layer dwelling planktonic foraminifera (Figure 2) from ODP Site 1052. These data indicate $\delta^{18}O$ changes of up to 1.4‰ in about 2500 to 4000 years. They attributed the high-amplitude $\delta^{18}O$ shifts to changes in sea surface temperatures (SSTs) of 4 to 10°C based on the presumed absence of significant ice sheets and hence little contribution from changes in the overall seawater $\delta^{18}O$ values.

[5] Such large temperature shifts present a significantly different view of the Eocene subtropics, thought to have been relatively stable compared to polar temperatures [e.g., *Pearson et al.*, 2007]. However, the magnitude of the temperature variations inferred from the Site 1052 $\delta^{18}O$ data is similar to that observed during the Pleistocene [*Kroon et al.*, 2000] suggesting that subtropical SSTs during relatively warm, and presumed ice-free climatic intervals could have exhibited the same magnitude of environmental change as during glacial-interglacial climates.

[6] The relatively large changes in SSTs were based on the assumption that the only source of foraminiferal $\delta^{18}O$ variations was seawater temperature. Yet recent evidence suggests that significant polar ice may have existed as far back as the late middle Eocene [e.g., *Eldrett et al.*, 2007; *St. John*, 2008] raising the possibility that some portion of the magnitude of the subtropical North Atlantic foraminiferal $\delta^{18}O$ variations could have been due to changes in the global seawater isotopic composition. Thus, the assumption that ice volume variations did not affect the foraminiferal $\delta^{18}O$ values changes at Blake Nose may have resulted in an overestimation of the magnitude of SST changes.

[7] To evaluate the magnitude of SST change at Site 1052, and better understand the nature of subprecessional-scale environmental change during the late middle Eocene, we present a high-resolution planktonic foraminiferal Mg/Ca record from ODP Site 1052 to complement the existing $\delta^{18}O$ data. Our interval also covers a major turnover in planktonic foraminifera with the extinction of muricate taxa *Morozovelloides* and *Acarinina* [*Wade*, 2004; *Wade et al.*, 2008]. The Mg/Ca ratios provide an independent estimate of SST indicating significant changes in the seawater $\delta^{18}O$ composition of the western subtropical North Atlantic not previously recognized.

2. Materials and Methods

2.1. Site Information

[8] Coring at ODP Site 1052 (Blake Nose, western North Atlantic, Figure 1) recovered middle to upper Eocene siliceous and nannofossil ooze [*Norris et al.*, 1998]. The modern water depth at Site 1052 is 1345 m. Given that middle-late Eocene sea level was ~100 m higher [e.g., *Miller et al.*, 2005] and Blake Nose had experienced most of its postrift subsidence by the end of the Early Cretaceous [*Norris et al.*, 1998], the paleo–sea level was likely within 100 m of the modern water depth. The study interval consists of relatively unconsolidated sediments and is found at relatively shallow burial depths (~80 to 120 m) because very little sediment has accumulated at Blake Nose since the end of the

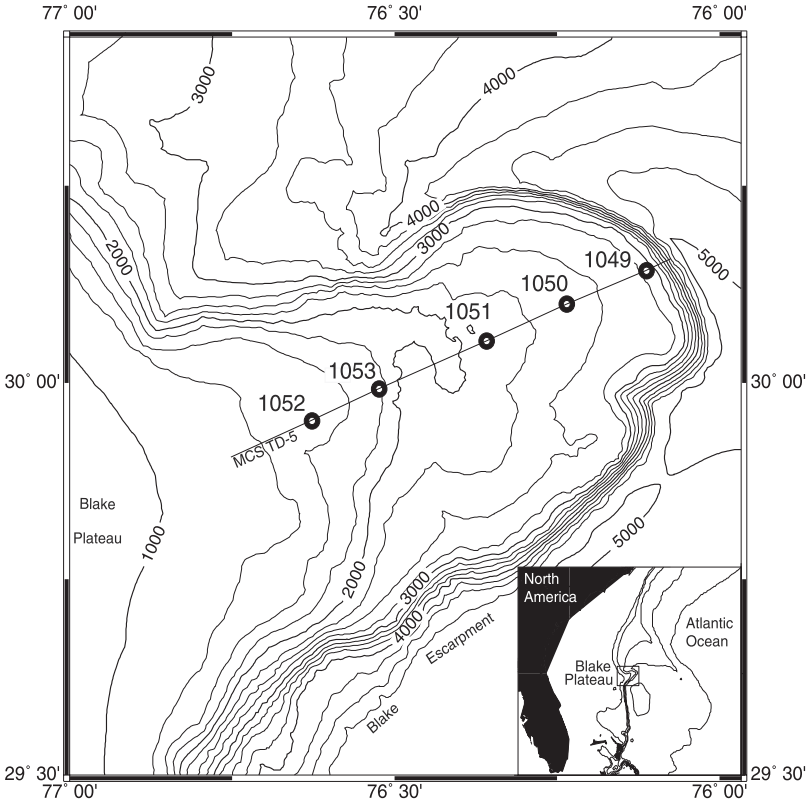

Figure 1. Location map showing drill locations and bathymetry (meters) of Ocean Drilling Program Leg 171B, Sites 1049–1053, and the Blake Plateau (inset) [*Norris et al.*, 1998].

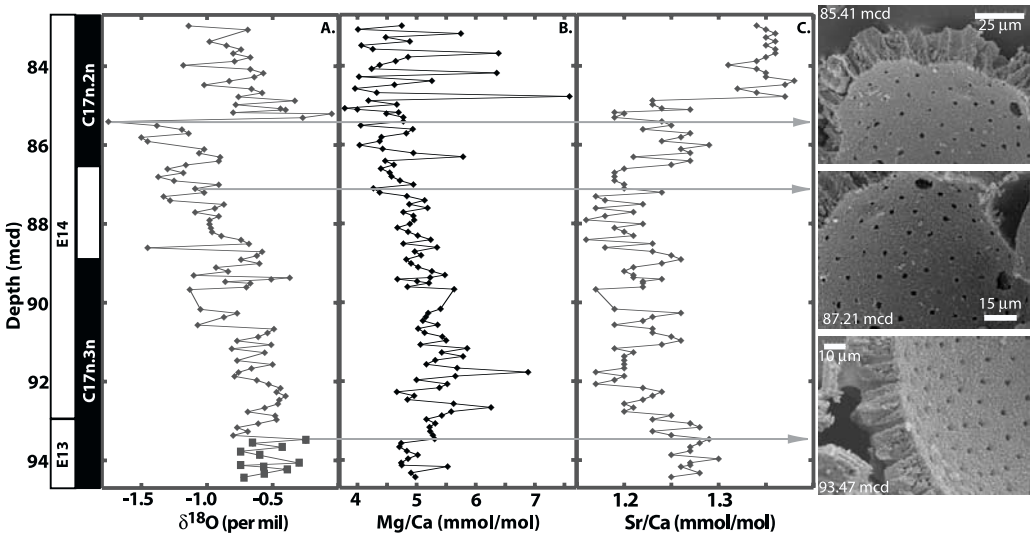

Figure 2. Comparison of Site 1052 geochemical data (plotted versus stratigraphic depth in mcd) and SEM images. (a) Site 1052 planktonic foraminiferal $\delta^{18}O$ data from *Wade and Kroon* [2002]. The diamond symbols indicate $\delta^{18}O$ analyses conducted on *Globigerinatheka* specimens, and the squares represent analyses of *Acarinina mcgowrani*. (b) Mg/Ca values generated in this study. All trace element data employed *Globigerinatheka* specimens. The four samples with Mg/Ca values >5.5 mmol/mol that occur above 85 mcd are likely anomalous and not representative of paleoenvironmental conditions; hence, these are not included in subsequent discussion of the paleoceanographic implications. (c) Sr/Ca data from Site 1052. SEM images of *Globigerinatheka* test wall texture from three samples (1052F, 10H-2, 115–116 cm; 1052F, 10H-3, 145–146 cm; and 1052B, 11H-5, 35–36 cm) are shown with the stratigraphic interval of each indicated by the long arrows. Scale bars vary and are indicated in each image. Planktonic foraminiferal biozones from *Wade* [2004] and magnetostratigraphy from *Norris et al.* [1998].

Eocene. Shipboard and postcruise microfossil investigations indicate that the calcareous fossil groups are well preserved [*Mita*, 2001; *Wade*, 2004; *Bellier et al.*, 2001; *Friedrich and Hemleben*, 2007].

[9] We analyzed 121 samples at 10 cm (about 2.5 to 4 ka) resolution over the interval 94.43–82.98 m composite depth (mcd; please refer to *Norris et al.* [1998] for details on how the mcd scale was constructed at Site 1052) (37.86–37.50 Ma) from ODP Site 1052 using the same sample intervals for Mg/Ca analysis as those used by *Wade and Kroon* [2002] for stable isotope analysis. We employed the age model used by *Wade and Kroon* [2002].

[10] The planktonic foraminiferal genus *Globigerinatheka* provided the best taxa for sea surface reconstruction among those genera present and sufficiently abundant for time series analysis during our study interval. The paleohabitat of *Globigerinatheka* has been inferred through multispecies $\delta^{18}O$ and $\delta^{13}C$ comparison [*Premoli Silva et al.*, 2006]. Middle and upper Eocene planktonic foraminifera stable isotope analyses indicate depleted $\delta^{18}O$ and enriched $\delta^{13}C$ in *Globigerinatheka* in comparison to the rest of the assemblage [*Boersma et al.*, 1987; *Wade*, 2004; *Sexton et al.*, 2006], indicative of a mixed layer habitat. Concurrent stable isotope measurements at Site 1052 indicate little (<0.3‰) offset in $\delta^{18}O$ between *Morozovelloides*, *Acarinina* and *Globigerinatheka* [*Wade and Kroon*, 2002; *Wade*, 2004]. *Globigerinatheka* probably occupied a mixed layer habitat and possessed endosymbionts and thus remained within the photic zone for the majority of their lifecycle. We therefore consider our Mg/Ca values to reflect mixed layer sea surface temperatures.

2.2. Mg/Ca as a Paleothermometer

[11] Mg/Ca ratios of modern planktonic foraminifera predominantly reflect the temperature of the water in which they calcified. The proportion of Mg in foraminiferal calcite increases with increasing temperature [*Delaney et al.*, 1985; *Nürnberg et al.*, 1996; *Elderfield and Ganssen*, 2000; *Lea et al.*, 2000; *Dekens et al.*, 2002; *Anand et al.*, 2003; *Barker et al.*, 2005]. *Anand et al.* [2003] derived a multispecies Mg/Ca temperature calibration for tropical and subtropical planktonic foraminifera, broadening the application of the Mg/Ca paleotemperature proxy beyond the earlier calibrations.

[12] Mg/Ca analyses paired with foraminiferal $\delta^{18}O$ values aid in extracting the relative contributions of seawater temperature from that of changes in the isotopic composition of seawater [e.g., *Lear et al.*, 2000; *Elderfield and Ganssen*, 2000]. Temperatures derived from the Mg/Ca values can be used to calculate the isotopic composition of seawater, and hence any ice volume or regional $\delta^{18}O_{sw}$ changes, from calcite $\delta^{18}O$ values.

[13] We employ the equation by *Anand et al.* [2003]:

$$Mg/Ca = 0.38\exp(0.09SST)$$

to estimate SSTs at ODP Site 1052 and we apply a middle Eocene seawater Mg/Ca ratio of 4.0 mmol/mol [*Wilkinson and Algeo*, 1989]. Our use of 4.0 for the seawater Mg/Ca value follows the detailed discussions presented by *Billups and Schrag* [2002], *Tripati et al.* [2003], and *Sexton et al.* [2006] among others, which highlight the uncertainty in estimating ancient oceanic Mg/Ca values. These studies calculated a range of water temperatures using different seawater values, ranging from an ancient value derived from the *Wilkinson and Algeo* [1989] curve to the modern value of 5.1. *Sexton et al.* [2006] demonstrated convincingly that the seawater estimates presented by *Stanley and Hardie* [1998], which are significantly lower than those of *Wilkinson and Algeo* [1989], result in calculated SSTs unrealistically high, even for the middle Eocene. Thus, they adopted a seawater Mg/Ca value of 3.9 mmol/mol. We incorporated a value of 4.0, which is slightly higher than that used by *Sexton et al.* [2006], because our study interval is later in the middle Eocene (both *Stanley and Hardie* [1998] and *Wilkinson and Algeo* [1989] curves indicate an increase in seawater Mg/Ca throughout the Cenozoic; thus, younger intervals were characterized by higher Mg/Ca). However, to illustrate the sensitivity of the SST calculation to the choice of seawater value, we calculated the difference in SST resulting from a seawater value of 3.9 versus 4.0. For a foraminiferal Mg/Ca value of 4.75 mmol/mol, the resulting SST at a seawater value of 3.9 mmol/mol is 31.11°C while at 4.0 mmol/mol is 30.82°C, a difference of ~0.3°C. Thus, the choice of seawater value affects the absolute value of calculated SST slightly, but does not affect the magnitude of relative SST changes inferred from the foraminiferal Mg/Ca data, nor does it impact interpretation of the results. We assume that the seawater value remained constant during our relatively short (~200 ka) study interval.

2.3. Analytical Details

[14] We picked 20 to 30 tests of specimens from the genus *Globigerinatheka* from the 250–355 μm

size fraction, and crushed and cleaned them using the standard rigorous reductive/oxidative cleaning protocol to remove the oxide coating and any residual organic material [e.g., *Boyle*, 1981; *Boyle and Keigwin*, 1985]. After cleaning, foraminiferal samples were analyzed with the Finnigan Element high-resolution ICP-MS at the Keck Elemental Geochemistry Laboratory, Department of Geological Sciences, University of Michigan. The total analytical uncertainty associated with the Mg/Ca measurements was 1.6% (r.s.d.) and 1.0% for Sr/Ca analyses. These relative standard deviations translate to ±0.08 for Mg/Ca and ±0.014 for Sr/Ca. Replicate analyses of Mg/Ca values (Table 1) yielded a standard deviation of 0.02 to 0.18. As indicated above, the 0.08 variation in Mg/Ca results in a calculated temperature uncertainty of 0.18°C; however, this value is negligible relative to the 1.2°C error based on uncertainty in the multispecies temperature calibration as reported by *Anand et al.* [2003]. Thus, we apply the calibration-associated error as an estimate of the maximum uncertainty, and recognize that while ±1.2°C indeed alters the absolute value of the estimated SST, this uncertainty does not change the trends or relative changes in the record, which are the focus of this work. This error in the calculated SST also affects the calculated $\delta^{18}O_{sw}$ values discussed in section 3.2. The analytical error associated with the Mg/Ca measurements combined with that for the published $\delta^{18}O_c$ values (0.09‰) [*Wade et al.*, 2001; *Wade and Kroon*, 2002], results in an uncertainty of ±0.14 on the $\delta^{18}O_{sw}$. However, the maximum uncertainty on the SST calculation translates to ±0.26 on the calculated $\delta^{18}O_{sw}$ value.

2.4. Foraminiferal Preservation

2.4.1. Scanning Electron Microscope Evaluation

[15] One potential cause of the short-term and high-amplitude changes in planktonic foraminiferal $\delta^{18}O$ is dissolution of primary calcite and precipitation of inorganic secondary calcite from pore fluids during diagenesis. Thus, we need to determine the effects of changes in diagenesis on the variations in the geochemical records. Selective dissolution of Mg-rich portions of the test and precipitation of diagenetic calcite from pore fluids potentially causes the Mg/Ca of a foraminiferal test to decrease and $\delta^{18}O_{calcite}$ values to increase [e.g., *Brown and Elderfield*, 1996; *Rosenthal et al.*, 2000]. The absolute effect of secondary calcite on the Mg/Ca and $\delta^{18}O$ of a foraminiferal test depends on the pore fluid composition and the burial conditions of the particular sedimentary interval.

[16] To exclude diagenesis as a cause of the variations in the proxy records, we examined foraminiferal specimens with a scanning electron microscope (Figure 2) at the Microscopy and Imaging Center (MIC) at Texas A&M University, targeting specimens specifically from intervals characterized by prominent shifts in $\delta^{18}O_{calcite}$ (arrows in Figure 2). Specimens indicate a frosty texture and recrystallization of the test walls, but there is no evidence of infilling. The frosty texture indicates that diagenesis likely affected the absolute $\delta^{18}O_{calcite}$ value. *Sexton et al.* [2006], however, found that while the $\delta^{18}O_{calcite}$ values of "frosty" planktonic foraminiferal specimens likely were altered, the Mg/Ca values were much less affected by the initial diagenetic alteration. Most importantly, the degree of recrystallization is consistent among all specimens analyzed, indicating that changes in preservation did not cause the prominent shifts in $\delta^{18}O_{calcite}$ values and likely did not introduce any bias into the trends or intersample variations in the Mg/Ca data.

2.4.2. Sr/Ca Measurements

[17] Sr/Ca data provides an additional gauge of preservation. Recrystallization from pore waters reduces Sr/Ca values in foraminiferal calcite [*Lorens and Bender*, 1980]; thus, diagenetically altered foraminifera should have lower Sr/Ca values than pristine samples [e.g., *Thomas et al.*, 1999]. Foraminiferal Sr/Ca analyses (Figure 2) indicate consistently high values (~1.2 mmol/mol) from the base of the studied interval (94.46 mcd) to 84.88 mcd, and then values increase to ~1.3 mmol/mol for the rest of the study interval. This increase is close to the prominent increase in $\delta^{18}O$ at 85.41 mcd; however, the changes do not coincide precisely. Furthermore, as stated above, there was no significant difference in the visual assessment of foraminiferal preservation across this interval of sharp increase. On the basis of the combination of SEM and geochemical indices we conclude that diagenesis had no significant influence on the variations in Mg and $\delta^{18}O$ contents of the foraminiferal tests and we interpret values and variations in terms of paleoceanographic conditions.

3. Results and Discussion

3.1. Mg/Ca Values and Paleotemperatures

[18] The planktonic foraminiferal Mg/Ca values range from 3.79 to 7.59 mmol/mol over the study

Table 1. Site 1052 Data and Sample Stratigraphic Information

Sample ID	Depth (mcd)	Age (Ma)	Mg/Ca (mmol/mol)	Sr/Ca (mmol/mol)	$\delta^{18}O$	SST	$\delta^{18}O_{sw}$
1052B-10-5,53-56[a]	82.98	37.505	4.75	1.34	−1.14	30.8	2.13
1052B-10-5,63-66	83.08	37.509	4.01	1.35	−0.69	28.9	2.18
1052B-10-5,73-76	83.18	37.513	5.75	1.36		32.9	
1052B-10-5,83-86	83.28	37.517	4.48	1.35		30.2	
1052B-10-5,93-96	83.38	37.521	4.89	1.36	−0.98	31.1	2.36
1052B-10-5,103-106	83.48	37.525	4.07	1.35	−0.85	29.1	2.06
1052B-10-5,113-116	83.58	37.529	4.26	1.36	−0.74	29.6	2.27
1052B-10-5,123-126	83.68	37.533	6.39	1.36	−0.80	34.1	3.16
1052B-10-5,133-136	83.78	37.537	4.86	1.35	−0.67	31.1	2.65
1052B-10-5,143-146	83.88	37.541	4.65	1.34	−0.79	30.6	2.43
1052B-10-6,3-6	83.98	37.545	4.38	1.31	−1.18	29.9	1.90
1052B-10-6,13-16	84.08	37.549	4.24	1.34	−0.67	29.6	2.33
1052B-10-6,23-26	84.18	37.553	6.36	1.35	−0.57	34.1	3.38
1052B-10-6,33-36	84.28	37.557	4.03	1.35	−0.64	29.0	2.24
1052B-10-6,43-46	84.38	37.561	5.26	1.38	−0.83	32.0	2.68
1052B-10-6,53-56	84.48	37.565	4.63	1.37	−1.02	30.5	2.19
1052B-10-6,63-66	84.58	37.568	3.96	1.32	−0.66	28.8	2.17
1052B-10-6,73-76	84.68	37.571	4.33	1.34	−0.58	29.8	2.47
1052B-10-6,83-86	84.78	37.574	7.59	1.37	−0.76	36.0	3.61
1052B-10-6,93-96	84.88	37.577	4.19	1.23	−0.33	29.4	2.64
1052B-10-6,103-106	84.98	37.579	4.67	1.23	−0.78	30.6	2.45
1052B-10-6,113-116	85.08	37.580	3.79	1.24	−0.44	28.3	2.30
1052F-10-2,83-86	85.11	37.583	4.00	1.27	−0.40	28.9	2.46
1052B-10-6,123-126	85.18	37.582	4.70	1.19	−0.80	30.7	2.45
1052F-10-2,9-96	85.21	37.585	4.49	1.20	−0.05	30.2	3.08
1052F-10-2,103-106	85.31	37.587	4.78	1.19	−0.27	30.9	3.01
1052F-10-2,113-116	85.41	37.587	4.78	1.24	−1.75	30.9	1.53
1052F-10-2,123-126	85.51	37.590	4.06	1.25	−1.38	29.1	1.52
1052F-10-2,133-136	85.61	37.592	4.94	1.22	−1.19	31.3	2.17
1052F-10-2,143-146	85.71	37.595	4.83	1.27	−1.14	31.0	2.17
1052F-10-3,3-6	85.81	37.598	4.41	1.26	−1.50	30.0	1.59
1052F-10-3,13-16	85.91	37.600	4.38	1.24	−1.45	29.9	1.63
1052F-10-3,23-26	86.01	37.603	4.04	1.29		29.0	
1052F-10-3,33-36	86.11	37.606	4.43	1.26	−1.02	30.0	2.08
1052F-10-3,43-46	86.21	37.608	4.95	1.27	−1.06	31.3	2.30
1052F-10-3,53-56	86.31	37.611	5.79	1.21	−0.90	33.0	2.83
1052F-10-3,63-66	86.41	37.614	4.47	1.27	−0.91	30.1	2.22
1052F-10-3,73-76	86.51	37.617	4.62	1.25	−1.16	30.5	2.05
1052F-10-3,83-86	86.61	37.619	4.40	1.20	−1.30	30.0	1.78
1052F-10-3,93-96	86.71	37.623	4.55	1.19	−1.18	30.3	1.99
1052F-10-3,103-106	86.81	37.627	4.58	1.19	−1.37	30.4	1.82
1052F-10-3,113-116	86.91	37.631	4.72	1.19	−1.25	30.8	2.00
1052F-10-3,123-126	87.01	37.634	4.95	1.20	−0.91	31.3	2.46
1052F-10-3,133-136	87.11	37.638	4.27	1.20	−1.09	29.6	1.93
1052F-10-3,143-146	87.21	37.642	4.38	1.24	−1.02	29.9	2.06
1052F-10-4,3-6	87.31	37.646	4.84	1.17	−1.33	31.0	1.98
1052F-10-4,13-16	87.41	37.649	5.14	1.18	−1.28	31.7	2.18
1052F-10-4,23-26	87.51	37.653	4.88	1.22	−0.87	31.1	2.47
1052F-10-4,33-36	87.61	37.656	5.19	1.17	−0.94	31.8	2.54
1052F-10-4,43-46	87.71	37.660	4.78	1.21	−1.09	30.9	2.20
1052F-10-4,53-56	87.81	37.663	4.95	1.18	−0.91	31.3	2.45
1052F-10-4,63-66	87.91	37.667	4.96	1.16	−0.98	31.3	2.40
1052F-10-4,73-76	88.01	37.671	4.89	1.22	−0.98	31.1	2.36
1052F-10-4,83-86	88.11	37.675	4.68	1.19	−0.97	30.7	2.27
1052F-10-4,93-96	88.21	37.679	4.86	1.20	−0.96	31.1	2.36
1052F-10-4,105-106	88.31	37.683	5.02	1.21	−0.89	31.4	2.51
1052F-10-4,113-116	88.41	37.687	5.24	1.16	−0.74	31.9	2.76
1052F-10-4,123-126	88.51	37.690	4.78	1.23	−0.68	30.9	2.61
1052F-10-4,133-136	88.61	37.693	5.35	1.18	−1.45	32.1	2.10
1052F-10-4,143-146	88.71	37.695	4.97	1.23	−0.58	31.3	2.80
1052F-10-5,3-6	88.81	37.698	5.08	1.25	−0.62	31.6	2.81
1052F-10-5,13-16	88.91	37.700	4.83	1.26	−0.74	31.0	2.57

Table 1. (continued)

Sample ID	Depth (mcd)	Age (Ma)	Mg/Ca (mmol/mol)	Sr/Ca (mmol/mol)	$\delta^{18}O$	SST	$\delta^{18}O_{sw}$
1052F-10-5,23-26	89.01	37.703	4.91	1.24	−0.60	31.2	2.75
1052F-10-5,33-36	89.11	37.705	5.03	1.21	−0.93	31.5	2.47
1052F-10-5,43-46	89.21	37.707	5.26	1.20	−0.84	32.0	2.67
1052F-10-5,53-56	89.31	37.710	5.48	1.21	−1.10	32.4	2.50
1052B-11-2,73-76	89.37	37.711	5.23	1.21	−0.37	31.9	3.13
1052F-10-5,63-66	89.41	37.712	4.68	1.24	−0.51	30.7	2.73
1052B-11-2,83-86	89.47	37.713	5.01	1.22	−0.86	31.4	2.53
1052F-10-5,73-76	89.51	37.715	5.21	1.22	−0.67	31.9	2.82
1052F-10-5,83-86	89.61	37.719	4.85	1.22	−0.70	31.1	2.62
1052B-11-2,103-106	89.67	37.719	5.64	1.17	−1.13	32.7	2.55
1052B-11-3,3-6	90.17	37.735	5.41	1.19	−1.05	32.3	2.53
1052B-11-3,13-16	90.27	37.738	5.20	1.26	−0.77	31.8	2.71
1052B-11-3,23-26	90.37	37.741	5.16	1.23	−0.87	31.7	2.59
1052B-11-3,33-36	90.47	37.744	5.11	1.22		31.6	
1052B-11-3,43-46	90.57	37.748	5.36	1.19	−1.07	32.2	2.48
1052B-11-3,53-56	90.67	37.751	5.03	1.23	−0.49	31.5	2.91
1052B-11-3,63-66	90.77	37.755	5.14	1.23	−0.54	31.7	2.92
1052B-11-3,73-76	90.87	37.758	5.44	1.25	−0.61	32.3	2.98
1052B-11-3,83-86	90.97	37.761	5.50	1.26	−0.77	32.5	2.84
1052B-11-3,93-96	91.07	37.764	5.07	1.24	−0.51	31.5	2.91
1052B-11-3,103-106	91.17	37.766	5.86	1.19	−0.81	33.2	2.95
1052B-11-3,113-116	91.27	37.768	5.43	1.21	−0.56	32.3	3.02
1052B-11-3,123-126	91.37	37.771	5.79	1.20		33.0	
1052B-11-3,133-136	91.47	37.773	5.32	1.20	−0.77	32.1	2.77
1052B-11-3,143-146	91.57	37.775	5.17	1.20	−0.50	31.8	2.97
1052B-11-4,3-6	91.67	37.778	5.69	1.20	−0.66	32.8	3.03
1052B-11-4,13-16	91.77	37.780	6.89	1.17	−0.76	35.0	3.39
1052B-11-4,23-26	91.87	37.783	5.66	1.20	−0.79	32.8	2.89
1052B-11-4,33-36	91.97	37.786	5.00	1.19	−0.62	31.4	2.77
1052B-11-4,43-46	92.07	37.789	5.52	1.17	−0.53	32.5	3.10
1052B-11-4,53-56	92.17	37.791	5.39	1.22	−0.44	32.2	3.13
1052B-11-4,63-66	92.27	37.794	4.67	1.24	−0.47	30.6	2.76
1052B-11-4,73-76	92.37	37.797	4.96	1.23	−0.40	31.3	2.97
1052B-11-4,83-86	92.47	37.799	4.85	1.22	−0.45	31.1	2.87
1052B-11-4,93-96	92.57	37.802	5.63	1.20	−0.46	32.7	3.21
1052B-11-4,103-106	92.67	37.805	6.26	1.21	−0.56	33.9	3.36
1052B-11-4,113-116	92.77	37.807	5.59	1.20	−0.69	32.6	2.96
1052B-11-4,123-126	92.87	37.810	5.43	1.25	−0.48	32.3	3.10
1052B-11-4,133-136	92.97	37.813	5.17	1.23	−0.47	31.8	3.00
1052B-11-4,143-146	93.07	37.815	5.32	1.27	−0.61	32.1	2.92
		37.815	5.16	1.27	−0.61	31.7	2.85
1052B-11-5,3-6	93.17	37.818	5.22	1.28	−0.77	31.9	2.72
		37.818	5.07	1.28	−0.77	31.5	2.65
1052B-11-5,13-16	93.27	37.821	5.23	1.23	−0.69	31.9	2.81
		37.821	4.99	1.26	−0.69	31.4	2.70
1052B-11-5,23-26	93.37	37.824	5.28	1.25	−0.80	32.0	2.71
		37.824	5.25	1.26	−0.80	31.9	2.70
1052B-11-5,33-36[b]	93.47	37.827	5.31	1.29	−0.25	32.1	3.28
		37.827	5.06	1.27	−0.25	31.5	3.17
1052B-11-5,43-46	93.57	37.830	4.74	1.28	−0.65	30.8	2.62
1052B-11-5,53-56	93.67	37.833	4.71	1.27	−0.43	30.7	2.82
1052B-11-5,63-66	93.77	37.836	4.84	1.27	−0.74	31.0	2.57
1052B-11-5,73-76	93.87	37.839	5.02	1.25	−0.60	31.4	2.80
1052B-11-5,83-86	93.97	37.842	4.86	1.30		31.1	
1052B-11-5,93-96	94.07	37.845	4.74	1.27	−0.30	30.8	2.96
1052F-11-1,113-116	94.13	37.846	4.75	1.27	−0.74	30.8	2.53
1052B-11-5,103-106	94.17	37.847	5.53	1.26	−0.57	32.5	3.06
1052F-11-1,123-126	94.23	37.849			−0.40		
1052F-11-1,133-136	94.33	37.852	4.91	1.28	−0.56	31.2	2.79
1052F-11-1,143-146	94.43	37.856	4.98	1.25	−0.72	31.3	2.66

[a] The $\delta^{18}O_{calcite}$ analyses of samples from 82.98 to 93.37 mcd used *Globigerinatheka* spp.
[b] The $\delta^{18}O_{calcite}$ analyses of samples from 93.47 to 94.43 mcd used *Acarinina mcgowrani*.

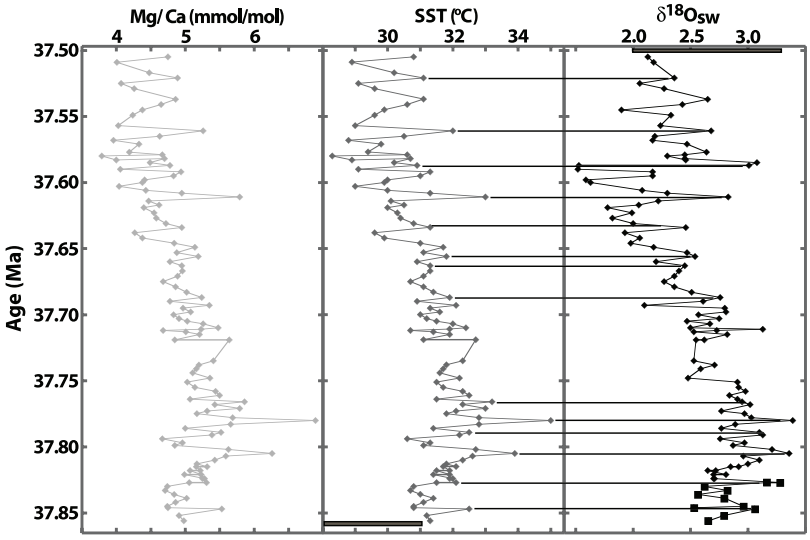

Figure 3. Mg/Ca values, calculated paleotemperatures, and calculated $\delta^{18}O_{sw}$ values plotted versus age. Black lines correlate short-term peaks in SST with peaks in $\delta^{18}O_{sw}$. The shaded rectangles in the second and third panels indicate the range of calculated paleotemperature and $\delta^{18}O_{sw}$, respectively, from *Sexton et al.* [2006] for 38 Ma.

interval (Table 1 and Figure 2). The first-order trend is an increase from ~5.0 mmol/mol at 94.43 mcd to ~5.7 mmol/mol at ~91.67 mcd (37.78 Ma), followed by a gradual decrease to ~4.8 mmol/mol at 82.98 mcd (Figure 2). Superimposed on these long-term trends are high-frequency variations of ~0.6 mmol/mol.

[19] Four samples (83.18, 83.68, 84.18, and 84.78 mcd) at the top of the interval had significantly and anomalously higher Mg/Ca values (Figure 2 and Table 1) than those recorded throughout the studied section. We suspect these anomalous values resulted from calcite loss (much smaller sample size) during the cleaning. Because they are anomalously high and do not correspond to any features in the $\delta^{18}O$ record [*Wade and Kroon*, 2002], we assume that these values do not reflect paleoenvironmental conditions, and we do not include them in our discussion of the paleoceanographic implications of the combined proxy data sets. Omitting these samples reduces the range in Mg/Ca values to 3.79 to 6.89.

[20] Sea surface temperatures estimated from the planktonic foraminiferal Mg/Ca values range from ~28 to 35°C (Figure 3). The long-term trend in the calculated temperature consists of an increase from ~31°C at 37.85 Ma to ~32°C at 37.82 Ma and then a decrease to ~29°C at 37.58 Ma, a cooling of ~3°C over 240 ka. In addition to the overall gradual decrease in temperature, the high-frequency variations in Mg/Ca record also indicate short-term variations in SST superimposed on the long-term trend. These variations correspond to shifts of ~0.8–1.5°C that occurred on a several ka time scale. It is interesting to note that the amplitude of temperature change estimated with Mg/Ca values is significantly lower than with $\delta^{18}O$ analyses, suggesting that factors in addition to temperature caused the prominent changes in foraminiferal $\delta^{18}O$.

[21] The reconstructed paleotemperatures from this study (~28–35°C) are similar to values from other middle- and low-latitude sites over this time interval (Figure 3). Paleotemperatures derived from the middle Eocene of Tanzania [*Pearson et al.*, 2001, 2007] range from 29 to 33°C, comparable to values obtained from this study. *Tripati et al.* [2003] reconstructed early Paleogene tropical temperatures from ODP Site 865 in the equatorial Pacific using planktonic foraminiferal Mg/Ca ratios and obtained a value of ~30°C at ~40 Ma. *Sexton et al.* [2006], in an attempt to assess the extent of diagenetic alteration in "frosty" planktonic foraminifera, compared the Mg/Ca of *Globigerinatheka* specimens from the middle Eocene of ODP sites 865 and 1052 to "glassy" foraminifera from Istra More 5 (Adriatic Sea). The Mg/Ca values (2.8–4.75 mmol/mol) they reported from ~38 Ma at ODP Site 1052 and the calculated temperatures (~25–31°C; applying the a seawater Mg/Ca value of 3.9 used by *Sexton et al.* [2006]) overlap with values from this study (Figure 3).

3.2. Isotopic Composition of Seawater ($\delta^{18}O_{sw}$)

[22] Mg/Ca derived temperature estimates can be used to constrain variations in the $\delta^{18}O$ of

seawater ($\delta^{18}O_{sw}$), enabling us to examine the possibility that ice volume or surface hydrography varied over the study interval. The $\delta^{18}O_{sw}$, expressed as the per mil deviation from the Standard Mean Ocean Water (SMOW) scale, is calculated by solving the quadratic equation for the $\delta^{18}O_{calcite}$ to temperature calibration of *Erez and Luz* [1983] and adding 0.27 to convert PDB to SMOW:

$$\delta^{18}O_{sw} = \delta^{18}O_c + 0.27 - ((4.52 - SQRT(18.3904 + .12T))/.06)$$

in which $\delta^{18}C_c$ is the isotopic composition of the foraminiferal calcite test referenced to the PDB standard (derived from the data set of *Wade et al.* [2001] and *Wade and Kroon* [2002]), $\delta^{18}O_{sw}$ is the isotopic composition of the seawater recorded by the surface mixed layer dwelling foraminifera, and T is temperature derived from Mg/Ca ratios (this study).

[23] The calculated $\delta^{18}O_{sw}$ indicates a long-term decrease from ~3‰ at 37.83 Ma to ~2‰ at 37.6 Ma (Figure 3). These values are higher than the current $\delta^{18}O_{sw}$ at Blake Nose (~1‰ [*LeGrande and Schmidt*, 2006]) but are comparable to $\delta^{18}O_{sw}$ values (~3.3 to 2.0‰) calculated from the Mg/Ca data of *Sexton et al.* [2006] using the same approach that we applied to our data set.

3.3. Implications and Causes of SST and $\delta^{18}O_{sw}$ Variations

[24] The combined Mg/Ca-derived paleotemperatures and calculated $\delta^{18}O_{sw}$ values indicate significant short- and long-term hydrographic variability. The SST record consists of short-term variations superimposed upon a long-term decrease over the course of the study interval (37.85–37.50 Ma). This long-term cooling is accompanied by a decrease in the $\delta^{18}O_{sw}$. The majority of the short-term fluctuations in SST and $\delta^{18}O_{sw}$ that occur on a ka time scale are also positively and significantly correlated (R = 0.66 in a linear regression of SST versus $\delta^{18}O_{sw}$); that is, maxima in temperature correspond to maxima in $\delta^{18}O_{sw}$ (Figure 3). Below we discuss the factors that may have caused this combination of long-term sea surface environmental variations, as well as the shorter-term fluctuations. Our data do not indicate a significant change in paleotemperatures or $\delta^{18}O_{sw}$ associated with the extinction of muricate taxa *Morozovelloides crassatus* and *Acarinina mcgowrani* at 92.37 and 92.77 mcd, respectively (Figure 3). This major turnover in planktonic foraminifera therefore does not appear to be climatically driven. Other factors, such as demise in photosymbiotic relationships [*Wade et al.*, 2008] may have been the causal mechanism.

3.3.1. Ice Volume

[25] The overall long-term decrease in SSTs coincides with a similar decrease in global deep water temperatures [e.g., *Zachos et al.*, 2001] and is consistent with a potential increase in or onset of continental ice expansion. However, the decrease in $\delta^{18}O_{sw}$ is the opposite trend expected for a build up of ice. While *St. John* [2008] recently reported evidence for the existence of Arctic sea ice as early as the middle Eocene (~46 Ma), and *Eldrett et al.* [2007] reported dropstones delivered by glacial ice as old as 38 Ma, our data suggests that changes in continental ice volume that may have been associated with ice rafting were not significant enough to alter $\delta^{18}O_{sw}$ values. *Burgess et al.* [2008] reached a similar conclusion for an earlier middle Eocene interval (~41 Ma) in a study of benthic and planktonic foraminiferal $\delta^{18}O$, Mg/Ca, and TEX_{86} analyses from the southwestern Pacific Ocean. However, given that global climate during the study interval was in the midst of the global cooling trend that culminated in the Eocene-Oligocene transition, we do not dispute the possibility that continental ice could have begun to increase gradually. For example, a subtle global ice volume effect could have existed but have been overprinted in the subtropics by more prominent local/regional hydrographic changes.

[26] The short-term variations in sea surface hydrography (e.g., the concomitant changes in SST and $\delta^{18}O_{sw}$) likely do not support a glacial mechanism for similar reasons: short-term warming that may have caused a decrease in glacial ice would have been accompanied by a decrease in $\delta^{18}O_{sw}$, and the opposite occurs in our data set.

3.3.2. Variations in the Gulf Stream and Upwelling

[27] Short-term variations in temperature and $\delta^{18}O_{sw}$ observed at Blake Nose (Figure 3) could be due to changes in local/regional hydrography. *Wade and Kroon* [2002] proposed fluctuations in the path of the proto–Gulf Stream as a cause of the high-amplitude SST changes (based on planktonic foraminiferal $\delta^{18}O$). We revisit this hypothesis here with the new Mg/Ca SST and reconstructed $\delta^{18}O_{sw}$ values. Modern western boundary currents constitute temperature and salinity anomalies relative to the surrounding water masses [e.g., *Levitus et al.*,

1994; *Levitus and Boyer*, 1994]. While the proto–Gulf Stream during the Eocene likely was not as strong a western boundary current as its modern counterpart due to the open Caribbean connection, *Watkins and Self-Trail* [2005] suggested that a Gulf Stream was present since at least the late Maastrichtian. *Pinet and Popenoe* [1985] inferred from seismic data that the position of the proto–Gulf Stream varied in the past. The inferred onshore-offshore shifts during the late middle Eocene could have resulted in several degrees of SST and significant $\delta^{18}O_{sw}$ change. Furthermore, the positive correlation within the combined SST and $\delta^{18}O_{sw}$ changes supports the hypothesis that changes in the influence of the western boundary current in the Blake Nose region caused the hydrographic changes. That is, a stronger influence of the proto–Gulf Stream at the study site should have caused higher temperatures and salinities (i.e., higher Mg/Ca and $\delta^{18}O_{sw}$ values), and vice versa.

[28] In addition to migration of the Gulf Stream track, changes in the distribution of proto–Gulf Stream eddies may have produced periodic hydrographic changes in the study region. Modern Gulf Stream eddies, usually 100–200 km in diameter, form from the cutoff of Gulf Stream meanders. The meanders grow and separate from the Gulf Stream and they migrate northward of the stream to form anticyclonic (warm-core) eddies and southward to form cyclonic (cold-core) eddies [*Richardson*, 1983]. Rings also move westward when they are not touching the Gulf Stream and eastward when they are attached to it [*Fuglister*, 1972; *Richardson*, 1983]. Since these rings have a different temperature and salinity signature from the surrounding water, their migration to surrounding areas could have contributed to the reconstructed variations in SST and $\delta^{18}O_{sw}$ at Blake Nose.

[29] Upwelling of colder waters is another potential cause of the short-term hydrographic variations at Blake Nose area, as previously suggested by *Wade et al.* [2000] to explain the $\delta^{18}O_{calcite}$ variations. Several climate model simulations [*Bice et al.*, 2000; *Huber and Sloan*, 2000] have predicted Ekman-driven upwelling along the eastern North Atlantic margin during the Eocene.

[30] Some combination of the three Gulf Stream–associated hydrographic changes (meanders, eddies, or upwelling) likely produced the recorded short-term changes in SST and $\delta^{18}O_{sw}$ at Blake Nose, and potentially could have contributed to the longer-term trends apparent in the records (e.g., a long-term shift in the pattern of the western boundary current). However, the long-term changes evident in the Mg/Ca and $\delta^{18}O_{sw}$ records may have resulted from a more global-scale process, and below we explore the potential role of the global hydrologic cycle.

3.3.3. Changes in the Hydrologic Cycle

[31] Surface water $\delta^{18}O$ can be influenced by factors such as evaporation, precipitation, atmospheric vapor transport and Rayleigh distillation. An excess of evaporation over precipitation (E-P) results in relatively high local/regional surface water $\delta^{18}O_{sw}$. Thus, regions characterized by high rates of evaporation, such as the subtropics, have higher $\delta^{18}O_{sw}$ values than regions characterized by high rates of precipitation, such as the ITCZ or polar regions.

[32] Results from the IODP Arctic coring expedition suggest that the early Eocene "greenhouse" interval was characterized by intensified hydrologic cycling [e.g., *Brinkhuis et al.*, 2006; *Pagani et al.*, 2006; *Sluijs et al.*, 2006]. This means that overall enhanced rates of evaporation, presumably from the subtropics, led to generally enhanced rates of precipitation at the poles. *Brinkhuis et al.* [2006] suggested episodes of increased freshening of Arctic surface waters during the early Eocene (~50 Ma) based on the presence of fresh water ferns *Azolla*. *Pagani et al.* [2006] found enriched δD of Arctic precipitation during the early Eocene due to decreased rainout during moisture transport from lower latitudes to the Arctic and increased moisture delivery to the Arctic. *Sluijs et al.* [2008] attributed increased sediment accumulation rates during the PETM in the Arctic Ocean to enhanced siliciclastic input by rivers in response to an intensification of the hydrological cycle.

[33] The late middle Eocene represents the most recent transition from a greenhouse to an icehouse climate. If high rates of hydrologic cycling characterized the greenhouse climate state, then the transitional interval should have been characterized by the decrease in overall hydrologic cycling. Such a decrease would have impacted the region of evaporation (the vapor source in the subtropics) as well as the region of ultimate precipitation (the high latitudes). The gradual long-term decrease in Site 1052 $\delta^{18}O_{sw}$ values over the study interval (Figure 3) may be evidence of the response of the subtropics to the general decline in hydrologic cycling. An overall decrease in the rate of evaporation would have been manifested as a decrease in the $\delta^{18}O_{sw}$ in the surface waters of the vapor source.

Thus, our data corroborate the hypothesis that the rate of global hydrologic cycling was higher during greenhouse climate intervals and lower during icehouse intervals.

4. Conclusions

[34] Middle Eocene planktonic foraminiferal Mg/Ca values from ODP Site 1052 reflect a gradual long-term decrease from 5.7 mmol/mol at ~37.8 Ma to 4.8 mmol/mol at ~37.5 Ma. This translates to a decrease in SSTs from ~32.8 to 30.8°C. $\delta^{18}O_{sw}$ values calculated using the Mg/Ca-estimated paleotemperatures decreased from ~3.0‰ at 37.8 Ma to ~2.1‰ at 37.5 Ma. Superimposed on the long-term trends are short-term (~ka scale) variations in both SSTs and the $\delta^{18}O_{sw}$. The short-term trends in the combined SST and $\delta^{18}O_{sw}$ data sets corroborate the hypothesis that variations in the Gulf Stream caused frequent and relatively high-amplitude sea surface hydrographical changes at Blake Nose. However, the long-term hydrographical changes at Blake Nose likely reflect weakening of global hydrologic cycling as the climate transitioned from a greenhouse to an icehouse.

Acknowledgments

[35] We gratefully acknowledge support to C. U. Okafor from the National Association of Black Geologists and Geophysicists for two grants that covered analytical expenses, as well as Scholarships from ConocoPhillips and Chevron awarded by the Department of Geology and Geophysics for salary support. We wish to thank Cedric John and Appy Sluijs for thoughtful and thorough reviews that improved the manuscript, as well as Vincent Salters for his service as Editor. The Ocean Drilling Program (ODP) provided samples from Blake Nose. The ODP is sponsored by the U.S. National Science Foundation and participating countries under management of the Joint Oceanographic Institutions Inc.

References

Adams, C. G., D. E. Lee, and B. R. Rosen (1991), Conflicting isotopic and biotic evidence for tropical sea-surface temperatures during the Tertiary, *Palaeogeogr. Palaeoclimatol. Palaeoecol.*, *77*, 289–313.

Anand, P., H. Elderfield, and M. H. Conte (2003), Calibration of Mg/Ca thermometry in planktonic foraminifera from a sediment trap time series, *Paleoceanography*, *18*(2), 1050, doi:10.1029/2002PA000846.

Barker, S., I. Cacho, H. Benway, and K. Tachikawa (2005), Planktonic foraminiferal Mg/Ca as a proxy for past oceanic temperatures: A methodological overview and data compilation for the last glacial maximum, *Quat. Sci. Rev.*, *24*, 821–834, doi:10.1016/j.quascirev.2004.07.016.

Bellier, J. P., M. Moullade, and B. T. Huber (2001), Mid-Cretaceous planktonic foraminifers from Blake Nose: Revised biostratigraphic framework [online], *Proc. Ocean Drill. Program Sci. Results*, *171B*, 12 pp. (Available at http://www-odp.tamu.edu/publications/171B_SR/VOLUME/CHAPTERS/SR171B03.PDF)

Bice, K. L., C. R. Scotese, D. Seidov, and E. J. Barron (2000), Quantifying the role of geographic change in Cenozoic ocean heat transport using uncoupled atmosphere and ocean models, *Palaeogeogr. Palaeoclimatol. Palaeoecol.*, *161*, 295–310, doi:10.1016/S0031-0182(00)00072-9.

Billups, K., and D. P. Schrag (2002), Paleotemperatures and ice volume of the past 27 Myr revisited with paired Mg/Ca and $^{18}O/^{16}O$ measurements on benthic foraminifera, *Paleoceanography*, *17*(1), 1003, doi:10.1029/2000PA000567.

Boersma, A., I. Premoli Silva, and N. J. Shackleton (1987), Atlantic Eocene planktonic foraminiferal paleohydrographic indicators and stable isotope paleoceanography, *Paleoceanography*, *2*, 287–331, doi:10.1029/PA002i003p00287.

Bohaty, S. M., and J. C. Zachos (2003), Significant Southern Ocean warming event in the late middle Eocene, *Geology*, *31*, 1017–1020, doi:10.1130/G19800.1.

Bohaty, S. M., J. C. Zachos, F. Florindo, and M. L. Delaney (2009), Coupled greenhouse warming and deep-sea acidification in the middle Eocene, *Paleoceanography*, *24*, PA2207, doi:10.1029/2008PA001676.

Boyle, E. A. (1981), Cadmium, zinc, copper and barium in foraminiferal test, *Earth Planet. Sci. Lett.*, *53*, 11–35, doi:10.1016/0012-821X(81)90022-4.

Boyle, E. A., and L. D. Keigwin (1985), Comparison of Atlantic and Pacific paleochemical records for the last 250,000 years: Changes in deep ocean circulation and chemical inventories, *Earth Planet. Sci. Lett.*, *76*, 135–150, doi:10.1016/0012-821X(85)90154-2.

Brinkhuis, H., et al. (2006), Episodic fresh surface waters in the Eocene Arctic Ocean, *Nature*, *441*, 606–609, doi:10.1038/nature04692.

Brown, S. J., and H. Elderfield (1996), Variations in Mg/Ca and Sr/Ca ratios of planktonic foraminifera caused by post-depositional dissolution: Evidence of shallow Mg-dependent dissolution, *Paleoceanography*, *11*, 543–551, doi:10.1029/96PA01491.

Burgess, C. E., P. N. Pearson, C. H. Lear, H. E. G. Morgans, L. Handley, R. D. Pancost, and S. Schouten (2008), Middle Eocene climate cyclicity in the southern Pacific: Implications for global ice volume, *Geology*, *36*, 651–654, doi:10.1130/G24762A.1.

Coxall, H. K., P. A. Wilson, H. Pälike, C. H. Lear, and J. Beckman (2005), Rapid stepwise onset of Antarctic glaciation and deep calcite compensation in the Pacific Ocean, *Nature*, *433*, 53–57, doi:10.1038/nature03135.

Dekens, P. S., D. W. Lea, D. K. Pak, and H. J. Spero (2002), Core top calibration of Mg/Ca in tropical foraminifera: Refining paleotemperature estimation, *Geochem. Geophys. Geosyst.*, *3*(4), 1022, doi:10.1029/2001GC000200.

Delaney, M. L., A. W. H. Be, and E. A. Boyle (1985), Li, Sr, Mg, Na in foraminiferal calcite shells from laboratory culture, sediment traps, and sediment cores, *Geochim. Cosmochim. Acta*, *49*, 1327–1341, doi:10.1016/0016-7037(85)90284-4.

Diester-Haass, L., and R. Zahn (1996), Eocene–Oligocene transition in the Southern Ocean: History of water mass circulation and biological productivity, *Geology*, *24*, 163–166, doi:10.1130/0091-7613(1996)024<0163:EOTITS>2.3.CO;2.

Elderfield, H., and G. Ganssen (2000), Past temperature and $\delta^{18}O$ of surface ocean waters inferred from foraminiferal Mg/Ca ratios, *Nature*, *405*, 422–445.

Eldrett, J. S., I. C. Harding, P. A. Wilson, E. Butler, and A. P. Roberts (2007), Continental ice in Greenland during the

Eocene and Oligocene, *Nature*, *446*, 176–179, doi:10.1038/nature05591.

Erez, J., and B. Luz (1983), Experimental paleotemperature equation for planktonic foraminifera, *Geochim. Cosmochim. Acta*, *47*, 1025–1031, doi:10.1016/0016-7037(83)90232-6.

Friedrich, O., and C. Hemleben (2007), Early Mastrichtian benthic foraminiferal assemblages from the western North Atlantic (Blake Nose) and their relation to paleoenvironmental changes, *Mar. Micropaleontol.*, *62*, 31–44, doi:10.1016/j.marmicro.2006.07.003.

Fuglister, F. C. (1972), Cyclonic rings formed by the Gulf Stream 1965–1966, in *Studies in Physical Oceanography: A tribute to George Wust on His 80th Birthday*, edited by A. Gordon, pp. 137–168, Gordon and Breach, New York.

Huber, M., and L. C. Sloan (2000), Climatic responses to tropical sea surface temperature changes on a "greenhouse" Earth, *Paleoceanography*, *15*, 443–450.

Kroon, D., J. J. G. Reijmer, and R. Rendle (2000), Mid- to late-Quaternary variations in the oxygen isotope signature of *Globigerinoides ruber* at Site 1006 in the western subtropical Atlantic, *Proc. Ocean Drill. Program Sci. Results*, *166*, 13–22.

Lea, D. W., D. K. Pak, and H. J. Spero (2000), Climate impact of late quaternary equatorial Pacific sea surface temperature variations, *Science*, *289*, 1719–1724, doi:10.1126/science.289.5485.1719.

Lear, C. H., H. Elderfield, and P. A. Wilson (2000), Cenozoic deep-sea temperatures and global ice volumes from Mg/Ca in benthic foraminiferal calcite, *Science*, *287*, 269–272, doi:10.1126/science.287.5451.269.

LeGrande, A. N., and G. A. Schmidt (2006), Global gridded data set of the oxygen isotopic composition in seawater, *Geophys. Res. Lett.*, *33*, L12604, doi:10.1029/2006GL026011.

Levitus, S., and T. P. Boyer (1994), *World Ocean Atlas 1994*, vol. 4, *Temperature, NOAA Atlas NESDIS*, vol. 4, 129 pp., NOAA, Silver Spring, Md.

Levitus, S., R. Burgett, and T. P. Boyer (1994), *World Ocean Atlas 1994*, vol. 3, *Salinity, NOAA Atlas NESDIS*, vol. 3, 111 pp., NOAA, Silver Spring, Md.

Lorens, R. B., and M. L. Bender (1980), The impact of solution chemistry on Mytilus edulis calcite and aragonite, *Geochim. Cosmochim. Acta*, *44*, 1265–1278, doi:10.1016/0016-7037(80)90087-3.

Miller, K. G., S. D. Wright, and R. G. Fairbanks (1991), Unlocking the ice-house: Oligocene-Miocene oxygen isotopes, eustasy, and margin erosion, *J. Geophys. Res.*, *96*, 6829–6848, doi:10.1029/90JB02015.

Miller, K. G., M. A. Kominz, J. V. Browning, J. D. Wright, G. S. Mountain, M. E. Katz, P. J. Sugarman, B. S. Cramer, N. Christie-Blick, and S. F. Pekar (2005), The Phanerozoic record of global sea-level change, *Science*, *312*, 1293–1298.

Mita, I. (2001), Data report: Early to late Eocene calcareous nannofossil assemblages of Sites 1051 and 1052, Blake Nose, northwestern Atlantic Ocean [online], *Proc. Ocean Drill. Program Sci. Results*, *171B*, 28 pp. (Available at http://www-odp.tamu.edu/publications/171B_SR/VOLUME/CHAPTERS/SR171B07.PDF)

Norris, R. D., et al. (1998), *Proceedings of the Ocean Drilling Program*, *Initial Reports*, vol. 171B, Ocean Drill. Program, College Station, Tex.

Nürnberg, D., J. Bijma, and C. Hemleben (1996), Assessing the reliability of magnesium in foraminiferal calcite as a proxy for water mass temperatures, *Geochim. Cosmochim. Acta*, *60*, 803–814, doi:10.1016/0016-7037(95)00446-7.

Pagani, M., et al. (2006), The Arctic's hydrological response to global warming during the Paleocene/Eocene thermal maximum, *Nature*, *442*, 671–675, doi:10.1038/nature05043.

Pearson, P. N., P. W. Ditchfield, J. Singano, K. G. Harcourt-Brown, C. J. Nicholas, R. K. Olsson, N. J. Shackleton, and M. A. Hall (2001), Warm tropical sea surface temperatures in the late Cretaceous and Eocene epochs, *Nature*, *413*, 481–487, doi:10.1038/35097000.

Pearson, P. N., B. E. van Dongen, C. J. Nicholas, R. D. Pancost, S. Schouten, J. M. Singano, and B. S. Wade (2007), Stable warm tropical climate through the Eocene epoch, *Geology*, *35*, 211–214, doi:10.1130/G23175A.1.

Pinet, P. R., and P. Popenoe (1985), A scenario of Mesozoic–Cenozoic ocean circulation over the Blake Plateau and its environs, *Geol. Soc. Am. Bull.*, *96*, 618–626, doi:10.1130/0016-7606(1985)96<618:ASOMOC>2.0.CO;2.

Premoli Silva, I., B. S. Wade, and P. N. Pearson (2006), Taxonomy, biostratigraphy, and phylogeny of *Globigerinatheka* and *Orbulinoides*, in *Atlas of Eocene Planktonic Foraminiferas*, *Spec. Publ. Cushman Found. Foraminiferal Res.*, *41*, 169–212.

Richardson, P. L. (1983), Gulf stream rings, in *Eddies in Marine Science*, edited by A. R. Robinson, pp. 19–45, Springer, Berlin.

Rosenthal, Y., G. P. Lohmann, K. C. Lohmann, and R. M. Sherrell (2000), Incorporation and Preservation of Mg in *Globigerinoides sacculifer*: Implications for Reconstructing the Temperature and $^{18}O/^{16}O$ of Seawater, *Paleoceanography*, *15*(1), 135–145.

Sexton, P., P. Wilson, and P. Pearson (2006), Microstructural and geochemical perspectives on planktic foraminiferal preservation: "Glassy" versus "frosty,", *Geochem. Geophys. Geosyst.*, *7*, Q12P19, doi:10.1029/2006GC001291.

Sluijs, A., et al. (2006), Subtropical Arctic Ocean temperatures during the Palaeocene/Eocene thermal maximum, *Nature*, *441*(7093), 610–613, doi:10.1038/nature04668.

Sluijs, A., U. Röhl, S. Schouten, H.-J. Brumsack, F. Sangiorgi, J. S. Sinninghe Damsté, and H. Brinkhuis (2008), Arctic late Paleocene–early Eocene paleoenvironments with special emphasis on the Paleocene-Eocene thermal maximum (Lomonosov Ridge, Integrated Ocean Drilling Program Expedition 302), *Paleoceanography*, *23*, PA1S11, doi:10.1029/2007PA001495.

Stanley, S. M., and L. A. Hardie (1998), Secular oscillations in the carbonate mineralogy of reef building and sediment-producing organisms driven by tectonically forced shifts in seawater chemistry, *Palaeogeogr. Palaeoclimatol. Palaeoecol.*, *144*, 3–19, doi:10.1016/S0031-0182(98)00109-6.

St. John, K. (2008), Cenozoic ice-rafting history of the central Arctic Ocean: Terrigenous sands on the Lomonosov Ridge, *Paleoceanography*, *23*, PA1S05, doi:10.1029/2007PA001483.

Thomas, D. J., T. J. Bralower, and J. C. Zachos (1999), New evidence for subtropical warming during the late Paleocene thermal maximum: Stable isotopes from Deep Sea Drilling Project Site 527, Walvis Ridge, *Paleoceanography*, *14*, 561–570, doi:10.1029/1999PA900031.

Tripati, A., M. L. Delaney, J. C. Zachos, L. D. Anderson, D. C. Kelly, and H. Elderfield (2003), Tropical sea-surface temperature reconstruction for the early Paleogene using Mg/Ca ratios of planktonic foraminifera, *Paleoceanography*, *18*(4), 1101, doi:10.1029/2003PA000937.

Wade, B. S. (2004), Planktonic foraminiferal biostratigraphy and mechanisms in the extinction of Morozovella in the late middle Eocene, *Mar. Micropaleontol.*, *51*, 23–38, doi:10.1016/j.marmicro.2003.09.001.

Wade, B. S., and D. Kroon (2002), Middle Eocene regional climate instability: Evidence from the western North

Atlantic, *Geology*, *30*, 1011–1014, doi:10.1130/0091-7613(2002)030<1011:MERCIE>2.0.CO;2.

Wade, B. S., D. Kroon, and R. D. Norris (2000), Upwelling in the late middle Eocene at Blake Nose?, *GFF*, *122*, 174–175.

Wade, B. S., D. Kroon, and R. D. Norris (2001), Orbitally forced climate change in the late middle Eocene at Blake Nose (Leg 171B): Evidence from stable isotopes, in *Western North Atlantic Palaeogene and Cretaceous Palaeoceanography Foraminifera*, edited by D. Kroon, R. D. Norris, and A. Klaus, *Geol. Soc. Spec. Publ.*, *183*, 273–291.

Wade, B. S., N. Al-Sabouni, C. Hemleben, and D. Kroon (2008), Symbiont bleaching in fossil planktonic foraminifera, *Evol. Ecol.*, *22*, 253–265, doi:10.1007/s10682-007-9176-6.

Watkins, D. K., and J. M. Self-Trail (2005), Calcareous nannofossil evidence for the existence of the Gulf Stream during the late Maastrichtian, *Paleoceanography*, *20*, PA3006, doi:10.1029/2004PA001121.

Wilkinson, B. H., and T. J. Algeo (1989), Sedimentary carbonate record of calcium-magnesium cycling, *Am. J. Sci.*, *289*, 1158–1194.

Wolfe, J. A. (1980), Tertiary climates and floristic relationships at high latitudes in the northern hemisphere, *Palaeogeogr. Palaeoclimatol. Palaeoecol.*, *30*, 313–323, doi:10.1016/0031-0182(80)90063-2.

Zachos, J. C., L. D. Stott, and K. C. Lohmann (1994), Evolution of early Cenozoic marine temperatures, *Paleoceanography*, *9*, 353–387, doi:10.1029/93PA03266.

Zachos, J. C., T. M. Quinn, and K. Salamy (1996), High resolution (10^4 yr) deep-sea foraminiferal stable isotope records of the Eocene–Oligocene climate transition, *Paleoceanography*, *11*, 251–266, doi:10.1029/96PA00571.

Zachos, J., M. Pagani, L. Sloan, E. Thomas, and K. Billups (2001), Trends, rhythms, and aberrations in global climate 65 Ma to present, *Science*, *292*, 686–693, doi:10.1126/science.1059412.